MicroNimbus: A Single-Chip 60 GHz SiGe Radiometer for Spaceborne Remote Sensing

Christopher T. Coen, Wyman Williams, and Nelson E. Lourenco
Advanced Concepts Laboratory
Georgia Tech Research Institute
Atlanta, GA 30332-0866
Email: christopher.coen@gtri.gatech.edu

Milad Frounchi, Clifford DY Cheon, and John D. Cressler
School of Electrical and Computer Engineering
Georgia Institute of Technology
Atlanta, GA 30332-0250
Email: cressler@ece.gatech.edu

***Abstract*—MicroNimbus is a 3U CubeSat under development at Georgia Tech that uses a 60 GHz radiometer to measure the temperature profile of the Earth's atmosphere. Due to the characteristics of oxygen absorption around 60 GHz, by choosing different center frequencies and bandwidths, the radiometer can measure the temperature of the atmosphere at different altitudes, giving the temperature profile. This is of interest to weather forecasters and workers in LIDAR and laser communications, among others. The radiometer front-end is implemented using a single SiGe MMIC that includes a front-end calibration switch, an LNA, an image-reject mixer with an integrated LO frequency quadrupler, an IF amplifier, and a synthesizer. The fabricated MMIC achieves 65 dB of conversion gain with a noise figure of 6.5 dB (4.3 dB without the switch) and an image rejection ratio of 31 dB. The required LO power is only -18 dBm and the total DC power is 180 mW. The low SWaP-C of this instrument would allow a constellation of such spacecraft to be deployed, yielding a continuous near-real-time 3-D map of the temperature profile of the Earth's atmosphere. All key components of the SiGe radiometer have been fabricated and tested, and the CubeSat bus design is currently at a CDR level.**

Keywords—radiometer; millimeter-wave integrated circuits, silicon germanium; cubesat

I. Introduction

The electromagnetic absorption of the Earth's atmosphere near 60 GHz is shown in Fig. 1(a) [1]. As can be seen here, the absorption spectrum consists of numerous discrete lines. At high altitudes (low pressure), the individual lines are distinct. Nearer to sea level, collisional broadening of the lines smears the spectrum into a broad band of absorption. By choosing appropriate center frequencies and bandwidths for the radiometer, the optical depth of the atmosphere therefore becomes "tunable." Table 1 shows an appropriate set of radiometer frequencies and bandwidths for constructing a temperature profilometer with seven altitude bins [2]. Fig. 1(b) shows the weighting functions for temperature measurements arising from this choice of center frequencies and bandwidths. This channelized approach lends itself naturally to a switched-filter radiometer implementation.

The goal of this work is to develop such a radiometer with size, weight, and power consumption (SWaP) that is compatible with the form factor of a 3U CubeSat. This radiometer should be suitable for low-cost scaled production to facilitate the development of a constellation of identical CubeSats that would enable continuous mapping of the Earth's atmospheric temperature. To accomplish these goals, the 60 GHz radiometer receiver is implemented on a single chip using a SiGe BiCMOS technology. SiGe heterojunction bipolar transistors (HBTs) are well-suited for CubeSat-based radiometers due to their high inherent tolerance to total-dose radiation, excellent $1/f$ noise properties, and compatibility with standard CMOS technologies on the same chip [5].

In this paper we present the radiometer and integrated SiGe MMIC developed for the MicroNimbus CubeSat. The MMIC contains all of the active microwave and millimeter-wave components in the system, including a front-end calibration switch, an LNA, a downconversion mixer, and a frequency synthesizer and quadrupler for driving the mixer. To the best of our knowledge, this level of radiometer integration at 60 GHz

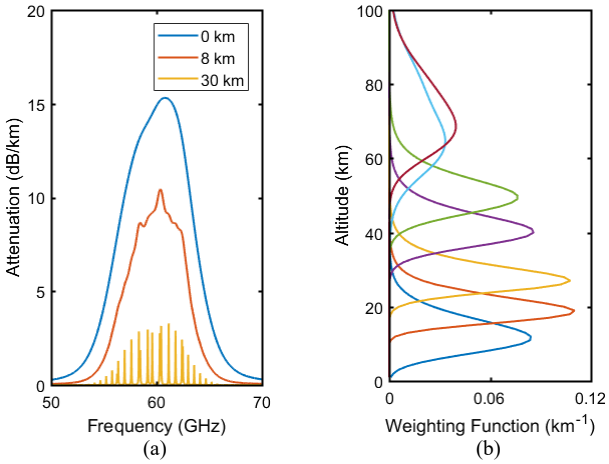

Fig. 1. (a) Absorption spectrum of oxygen at various altitudes in the Earth's atmosphere and (b) altitude bins for the temperature profilometer [3, 4].

TABLE I. CHANNEL SELECTIONS FOR ALTITUDE WINDOWS [3, 4]

Channel Number	Center Freq. (GHz)	Bandwidth (MHz)	Altitude Window (km)	Window Width (km)
1	64.47	200	12	11
2	60.82	200	18	7
3	58.388	30	27	9
4	60.4409	2.5	40	12
5	60.4365	1	50	20
6	63.5686	1.5	60	21
7	60.4348	1.5	73	20

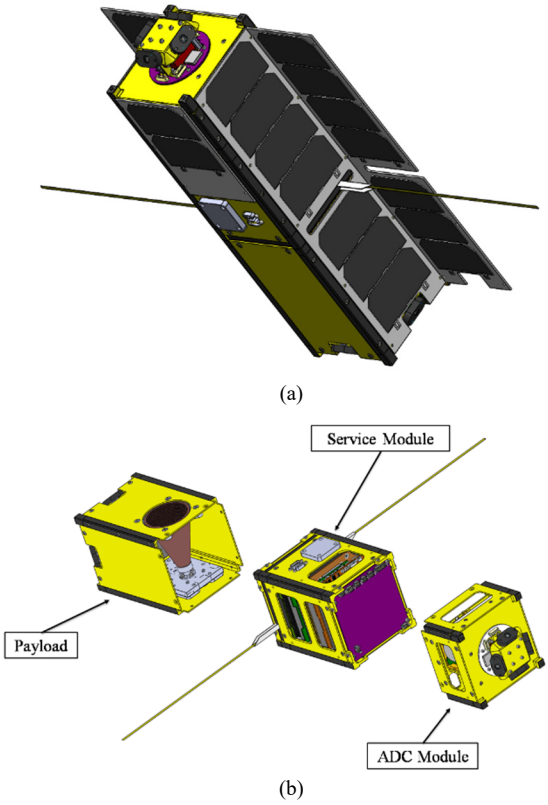

Fig. 2. (a) Isometric view of the MicroNimbus CubeSat. (b) Exploded view of the CubeSat showing the major sub-modules.

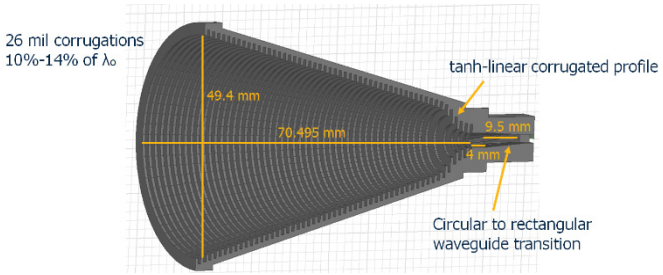

Fig. 3. Model of the V-band corrugated horn antenna for the MicroNimbus radiometer.

has not been achieved previously. This work is the result of a three-year IR&D effort between the Georgia Tech Research Institute and the Georgia Institute of Technology [3].

II. System Overview

Fig. 2 shows the current CAD design of the profilometer CubeSat, which has been named MicroNimbus as an homage to the Nimbus series of spacecraft that flew microwave radiometers for NASA in the 1970s. The bottom 1.5U (10 cm × 10 cm × 15 cm) of the 3U (10 cm × 10 cm × 30 cm) CubeSat is the radiometer payload. The Service Module contains the Command and Data Handling, Communications, Electrical Power System, and Navigation subsystems. The Attitude Determination and Control (ADC) Module contains a set of four sun sensors, three reaction wheels, three magnetic torque rods, and an inertial measurement unit (IMU). Another four sun sensors are in the payload module. Using all of these components, the ADC

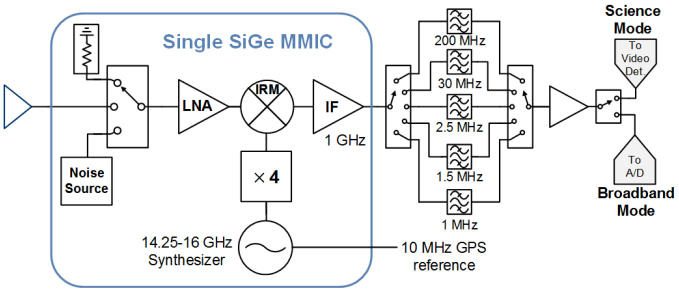

Fig. 4. Simplified block diagram of the MicroNimbus instrument.

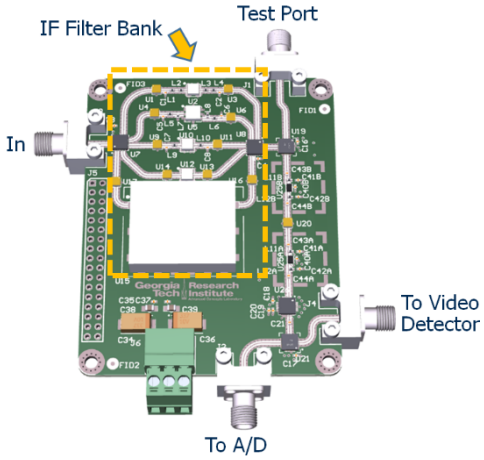

Fig. 5. Back-end IF electronics for the MicroNimbus radiometer.

subsystem de-tumbles the spacecraft, maintains 3-axis stability and keeps its antenna pointed at nadir with at most 1° of pointing error.

The antenna was designed for an 8° beamwidth which, from a 411 km orbit, gives a 57 km diameter field of view on the atmosphere. Fifty-seven km is approximately 0.5° of latitude and longitude, a popular resolution for weather model data published by NOAA. Considerations of atmospheric drag and solar panel usage necessitate that MicroNimbus flies with one of its 10 cm × 10 cm faces pointed in the direction of motion. The antenna must therefore look out of one of the 10 cm × 30 cm faces and is therefore constrained to a maximum length of less than 10 cm. The antenna, shown in Fig. 3, achieved the required 8° beamwidth within this short length by using a corrugated feedhorn design with a tanh-linear corrugated profile near the waveguide feed.

A block diagram of the radiometer is shown in Fig. 4. The first block in the SiGe MMIC is a low-loss calibration switch which frequently calibrates the radiometer by alternately connecting an ambient-temperature load and an active noise source to the receiver input. The core of the receiver consists of a 58–65 GHz low-noise amplifier, a wideband mixer, and a 1 GHz IF amplifier. Due to the low IF, the mixer must provide image rejection to ensure no noise energy from the lower mixer sideband is mixed with the noise from the desired channel. The mixer is driven by an on-chip frequency quadrupler and a phase-locked synthesizer. As can be seen from Table 1, operation of the radiometer requires very precise selection of the radiometer's operating frequency. Therefore, the synthesizer is phase locked

TABLE II. REQUIRED INTEGRATION TIMES FOR GIVEN ΔT_{RMS} VALUES

	ΔT_{RMS} (K)		
Channel BW	0.5	1	2
1 MHz	8.410 s	2.103 s	0.526 s
1.5 MHz	5.607 s	1.402 s	0.350 s
2.5 MHz	3.364 s	0.841 s	0.210 s
30 MHz	0.280 s	0.070 s	0.018 s
200 MHz	0.042 s	0.011 s	0.003 s
Total τ	23.352 s	5.838 s	1.459 s

to a frequency reference derived from a GPS receiver to achieve this precise tuning.

The radiometer steps between altitude windows by synchronously adjusting the synthesizer frequency and selecting the appropriate filter from an off-chip bank of COTS filters. As shown in Fig. 5, the IF electronics board consists of the switched filter bank along with IF amplifiers and a mode selection switch. In the nominal "science mode" of operation the filtered noise is input to a square-law detector. However, the back-end can be switched to "broadband mode" to digitize arbitrary 60 GHz waveforms of interest in space. Separate detection and digitization electronics are used for each mode of operation.

The temperature resolution of a total-power radiometer is given by

$$\Delta T_{RMS} = (T_{ANT} + T_{REC})\sqrt{\frac{1}{B\tau} + \left(\frac{\Delta G}{G}\right)^2} \qquad (1)$$

where T_{ANT} is the antenna noise temperature (assumed to be 150 K), T_{REC} is the receiver noise temperature (measured 1300 K noise temperature of the MMIC), B is the system bandwidth, and τ is the integration time. The $\Delta G/G$ term accounts for uncertainty due to short-term and long-term receiver gain fluctuations, which are primarily caused by $1/f$ noise in the receiver. This receiver could be operated in the Dicke mode to remove this term from the equation, although at a 2x penalty to ΔT_{RMS}. SiGe HBTs, however, have extremely low $1/f$ noise and do not exhibit significant gain fluctuations [6, 7]. To take advantage of this characteristic, we plan to operate the radiometer in total-power mode and tolerate small short-term gain fluctuations. The receiver will be calibrated periodically as required to correct for more significant long-term fluctuations.

Traveling at 7.7 km/s, MicroNimbus will traverse a 57 km spot in 7.5 s. Therefore, during its 7.5 s measurement window, the radiometer must make two measurements at a 200 MHz bandwidth, two at 1.5 MHz, and one each at 1 MHz, 2.5 MHz and 30 MHz. As shown in Table 2, the narrowest-band measurements require the greatest integration time to achieve a given ΔT_{RMS}—the two measurements with 1.5 MHz bandwidth and the one with 1 MHz bandwidth together consume 84% of the total measurement time. Assuming a receiver noise temperature of 1300 K, the radiometer can make its seven required measurements with a ΔT_{RMS} of 1 K in a total of 5.838 s.

III. SIGE RADIOMETER MMIC

The SiGe MMIC is designed in the GlobalFoundries BiCMOS8XP technology, which offers 0.13 µm CMOS devices along with SiGe HBTs with peak f_T/f_{max} values of 250/330 GHz.

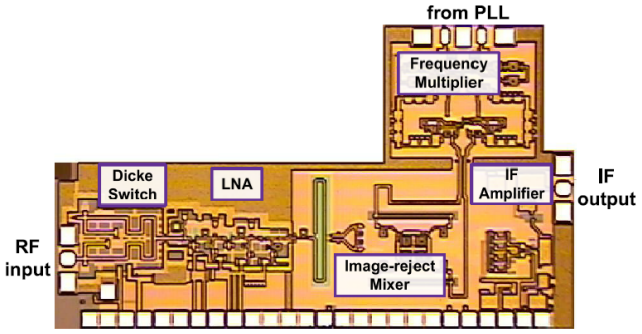

Fig. 6. Die photograph of the current SiGe receiver MMIC. The chip occupies an area of 3.1 mm^2 and consumes 180 mW of DC power [4].

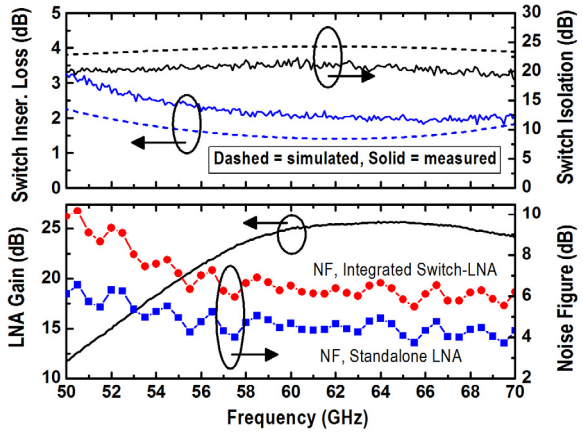

Fig. 7. Measured performance of the SPDT switch, LNA, and integrated switch-LNA in the SiGe receiver MMIC [3].

Each circuit block was designed and optimized specifically for this application, targeting a low receiver noise temperature with minimal power consumption. All of the key components of the SiGe MMIC have been designed and tested. A die photograph of the most recently tested version of the SiGe MMIC is shown in Fig. 6 [4]. The MMIC contains a digitally-controlled single-pole double-throw (SPDT) switch, an LNA, an image-reject mixer with an LO frequency quadrupler, and a 1 GHz IF amplifier.

The SPDT switch was designed using a standard quarter-wave shunt topology. SiGe HBTs in the reverse-saturated configuration were used as the switching devices to achieve a high off-state resistance and low insertion loss [8]. One input of the switch was connected to the RF input of the MMIC, while the other was connected to an on-chip 50 Ω load implemented using a thin-film TaN resistor. Large CMOS inverters are used to supply the base current to the switching SiGe HBTs, and the switch is controlled by a single digital bit. The switch achieves 2.0 dB of insertion loss and 21 dB of isolation, as shown in the top half of Fig. 7.

The SiGe LNA was designed to achieve 25–30 dB of gain across the 58–65 GHz instrument bandwidth. The design uses two cascode stages followed by a single common-emitter stage to achieve a wideband output match. Each amplification stage uses inductive emitter degeneration to achieve low noise without significantly trading off gain, and each transistor is implemented using an optimal-f_{max} emitter length of 6 µm to maximize the

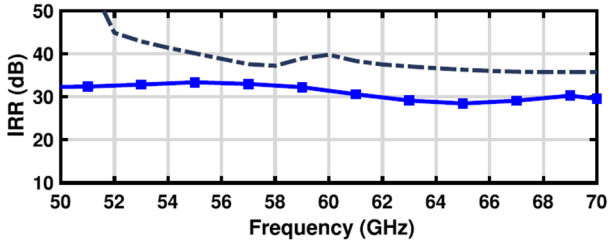

Fig. 8. Measured IRR of the SiGe image-reject mixer. The solid trace is measured and dashed trace is simulated [4].

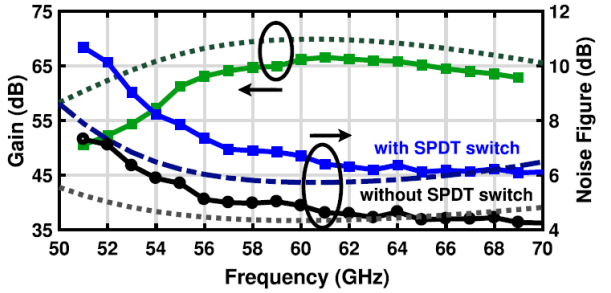

Fig. 9. Measured (solid) and simulated (dashed) gain and noise figure of the integrated SiGe receiver [4].

gain of each SiGe HBT. Current mirrors are included on chip to simplify the biasing of the LNA, and RC networks are used on all bias lines to ensure stable operation at both low and high frequencies. All matching networks were implemented using compact spiral inductors and capacitors to ensure a small layout. As shown in Fig. 7, the LNA achieves a peak gain of 25.6 dB at 65 GHz with a mean noise figure (NF) of 4.6 dB across the band. When integrated with the switch, the mean NF increases to 6.4 dB. The power consumption is only 20 mW from a single 1.5 V supply.

The image-reject mixer in the MMIC enables the use of a single-conversion radiometer receiver. The active mixer is implemented using a double-balanced Gilbert cell topology to achieve a small core size, excellent LO-to-IF isolation, and conversion gain instead of loss. A Marchand balun is used to convert the single-ended LNA output to the differential input of the mixer. Quadrature hybrids and a low-loss polyphase network with resonating inductors are used to supply the differential quadrature LO signals to the transistor core [4, 9]. The IF network uses a lumped polyphase filter with a differential active combiner to return to single-ended operation. As shown in Fig. 8, the mixer achieves a mean image rejection ratio (IRR) of 31 dB across 50–70 GHz. The mixer is followed by a simple two-stage resistive feedback IF amplifier which provides 40 dB of IF gain.

The integrated radiometer MMIC achieves 65 dB of conversion gain with a mean NF of 6.5 dB across the band, as shown in Fig. 9. The mixer is driven by an on-chip frequency quadrupler that consists of two cascaded frequency doublers. Each doubler uses a bootstrapped Gilbert cell topology to achieve a high conversion gain, low input power, and low output imbalance [10]. The quadrupler has a measured output power of +6 dBm with a conversion gain of 19 dB, and the DC power consumption is 75 mW. The integrated MMIC consumes

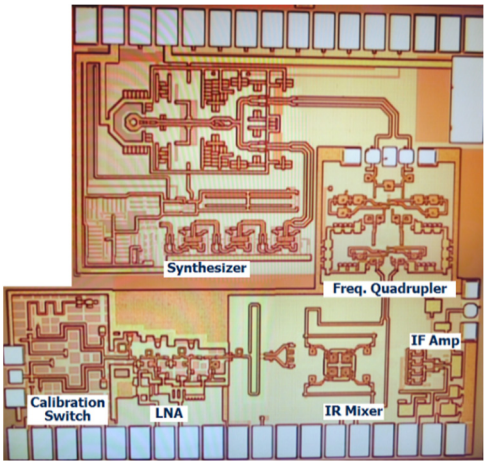

Fig. 10. Die photograph of the fully integrated radiometer MMIC. The chip dimensions are 2.70 mm × 2.90 mm.

180 mW of DC power and requires a low LO drive power of only -19 dBm at around 15 GHz

The fully integrated version of the MMIC, shown in Fig. 10, recently returned from fabrication and is awaiting characterization. The building blocks of the synthesizer (VCO, prescaler and CMOS divider) are implemented using SiGe HBTs and CMOS, and all CMOS structures are laid out in a manner that will prevent single-event latchup events. The fully integrated MMIC also includes a full front-end calibration switch instead of a Dicke switch. This calibration switch replaces the quarter-wave lines in the Dicke switch with 14 dB directional couplers implemented in edge-coupled microstrip. A weakly coupled SiGe HBT-based avalanche noise source injects an excess noise temperature of 600 K into the receiver input. This noise source, along with the on-chip temperature-monitored load, enables rapid and frequent calibration of the radiometer. Additional results for this final MMIC will be presented with the poster.

IV. Conclusions

The MicroNimbus spacecraft will provide atmospheric temperature profile data at an altitude resolution of 10 km, a geographic resolution of 0.5° longitude and latitude, and a temperature resolution of 1 K RMS. The SiGe receiver MMIC developed under this work significantly reduces SWaP compared to traditional mm-wave radiometers and facilitates low-cost scale production for envisioned CubeSat constellations.

Acknowledgment

The authors are grateful to Prof. Glenn Lightsey, Tanish Himani, Terry Stevenson, and Andrew Fear from the Space Systems Design Lab at Georgia Tech and Amanda Belding, Phil Bowden, Kathy Bowland, and Annie Jones-Wyatt from GTRI for their contributions. We thank GTRI for supporting this effort on IR&D and GlobalFoundries for chip fabrication.

References

[1] M. L. Meeks and A. E. Lilley, “The Microwave Spectrum of Oxygen in the Earth's Atmosphere,” *J. Geophysical Research*, vol. 68, no. 6, pp. 1683–1703, Mar. 1963.

[2] W. B. Lenoir, “Remote Sounding of the Upper Atmosphere by Microwave Measurements,” Ph.D. Thesis, Massachusetts Institute of Technology, Cambridge, MA, May 1965.

[3] W. Williams, C. Coen, M. Frounchi, N. Lourenco, and J. D. Cressler, “MicroNimbus: A CubeSat Temperature Profilometer for the Earth's Atmosphere Using a Single-Chip 60 GHz SiGe Radiometer,” *Proc. IEEE Int. Geosci. Remote Sens. Symp.,* 2017, pp. 2740–2743.

[4] M. Frounchi, C. Coen, C. Cheon, N. Lourenco, W. Williams, and J. D. Cressler, “A V-band SiGe Image-Reject Receiver Front-End for Atmospheric Remote Sensing,” *Proc. IEEE BiCMOS and Compound Semicond. Integr. Circuits and Technol. Symp.*, Oct. 2018, pp. 223–226.

[5] C. T. Coen, J. R. Piepmeier, and J. D. Cressler, “Integrated Silicon-Germanium Electronics for CubeSat-Based Radiometers,” *IEEE Int. Geosci. Remote Sens. Symp.*, 2013, pp. 1286–1289.

[6] J. D. Cressler and G. Niu, *Silicon-Germanium Heterojunction Bipolar Transistors*. Norwood, MA: Artech House, 2003.

[7] S. Weinreb and J. Schleeh, "Multiplicative and Additive Low-Frequency Noise in Microwave Transistors," *IEEE Trans. Microw. Theory Techn.*, vol. 62, no. 1, pp. 83-91, Jan. 2014.

[8] R. L. Schmid, P. Song, C. T. Coen, A. Ç. Ulusoy and J. D. Cressler, "On the Analysis and Design of Low-Loss Single-Pole Double-Throw W-Band Switches Utilizing Saturated SiGe HBTs," *IEEE Trans. Microw. Theory Techn.*, vol. 62, no. 11, pp. 2755-2767, Nov. 2014.

[9] M. Frounchi, A. Alizadeh, C. T. Coen, and J. D. Cressler, “A Low-Loss Broadband Quadrature Signal Generation Network for High Image Rejection at Millimeter-Wave Frequencies,” *IEEE Trans. Microw. Theory Techn.*, vol. 66, no. 12, pp. 5336–5346, Dec. 2018.

[10] M. Frounchi, S. G. Rao, and J. D. Cressler, “A Ka-Band SiGe Bootstrapped Gilbert Frequency Doubler With 26.2% PAE,” *IEEE Microw. Compon. Lett.*, vol. 28, no. 12, pp. 1122–1124, Dec. 2018.